Quantum cascade semiconductor infrared and far-infrared lasers: from trace gas sensing to non-linear optics

Geoffrey Duxbury,* Nigel Langford, Michael T. McCulloch and Stephen Wright

Received 18th January 2005
First published as an Advance Article on the web 19th April 2005
DOI: 10.1039/b400914m

The Quantum cascade (QC) laser is an entirely new type of semiconductor device in which the laser wavelength depends on the band-gap engineering. It can be made to operate over a much larger range than lead salt lasers, covering significant parts of both the infrared and submillimetre regions, and with higher output power.
In this *tutorial review* we survey some of the applications of these new lasers, which range from trace gas detection for atmospheric or medical purposes to sub-Doppler and time dependent non-linear spectroscopy.

Department of Physics, University of Strathclyde, John Anderson Building, 107 Rottenrow, Glasgow, UK G4 0NG

Geoffrey Duxbury

Geoffrey Duxbury was born in 1942 in Blackburn, Lancashire, and is a Professor of Chemical Physics in the Department of Physics at Strathclyde University. He obtained BSc (1964) and PhD (1967) degrees from Sheffield University. After a Junior Research Fellowship at the National Physical Laboratory he joined the Theoretical Chemistry Department at Bristol University in 1970, becoming a lecturer in Chemical Physics in 1975. In 1981 he moved to Strathclyde University. He was awarded the Marlow Medal of the Faraday Division of the Royal Society of Chemistry in 1975, and was elected a Fellow of the Royal Society of Edinburgh in 1997. His current research is in the application of molecular spectroscopy to atmospheric chemistry and physics and to non-linear optics.

Nigel Langford

Nigel Langford was born in Hull, in 1962, and is a Senior Lecturer in the Department of Physics at the University of Strathclyde. He obtained BSc (1983) and PhD (1988) degrees from the Imperial College London. Following post-doctoral work at the Universities of St Andrews, Toronto and Strathclyde, he held an ESPRC Advanced Fellowship from 01 Jan 1992–30 Dec 1996. He was appointed Lecturer in 1992 and Senior Lecturer in 1999. His research interests are in laser physics and laser spectroscopy, ranging from ultrafast spectroscopy to the development of fibre laser and QC laser spectrometers.

Michael McCulloch

Michael McCulloch obtained a BSc in Physics at Strathclyde University in 2001, and having completed his PhD thesis in 2004 is working as a Physicist in Cascade Technologies Ltd. His PhD research was concerned with the development and testing of an infrared intra-pulse quantum cascade laser spectrometer and its application to trace gas detection and to non-linear optics. This involved both the modelling of the performance of the spectrometer and also the design of much of its control and data acquisition system.

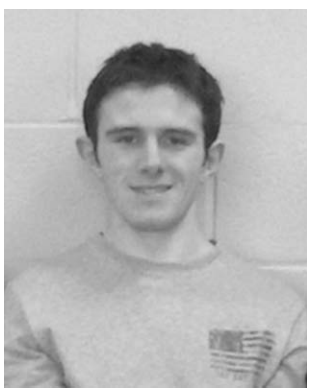

Stephen Wright

Stephen Wright obtained a BSc in Physics at Strathclyde University in 2003 and is currently studying for a PhD. His research, funded by the NERC COSMAS programme, is concerned with developing the intra-pulse QC laser spectrometer for deployment in field measurements and for aircraft borne operation to detect atmospheric trace gases.

Introduction

Tuneable mid-infrared diode lasers have been used for molecular spectroscopy for over thirty years. In 1974 the MIT Lincoln Laboratory group of Hinkley, Knill and Blum[1] published a review article describing a variety of uses for spectrometers based upon tuneable diode lasers such as line broadening measurements, molecular beam spectroscopy and atmospheric measurements. This set the stage for the many uses of these spectrometers in the intervening period. Since infrared diode laser spectroscopy appears to be such a mature field it might be wondered why a particular type of diode laser, the quantum cascade laser (QC), can make a significant impact on mid infrared molecular spectroscopy, given the range of applications developed since the pioneering work of the Lincoln Laboratory group.

The mid infrared diode lasers developed at the Lincoln Laboratory were direct band-gap lasers. In designing these lasers, a semiconductor material is selected in which the energy separation of the band gap between the valence and the conduction bands is such that, when positive holes (p) and negative electrons (n) recombine, energy is emitted at the appropriate wavelength. This is known as a p-n junction device or alternatively a bipolar laser. The materials used for these lasers are varieties of lead salts, such as the ternary systems $Pb_{1-x}Sn_xTe$ and $Pb_{1-x}Sn_xSe$. These lasers may be produced to cover a wide wavelength range, and an individual device may have a wide tuning range when a combination of temperature and current tuning is used. Their main disadvantages are that they must be operated at cryogenic temperatures (initially 8–50 K, more recently 77 K), their power output is usually low, microwatts, and their beam quality is quite variable. In some wavelength regions[2,3] groups have replaced the use of lead salt diode lasers by non-linear frequency conversion techniques such as difference frequency generation of tuneable infrared radiation, or optical parametric oscillators. These instruments use widely tuneable dye or solid state lasers such as a titanium sapphire to give broadband coverage with good beam quality. They are inherently low power, and are very dependent upon having an efficient non-linear mixing crystal for the desired wavelength region.

The region for which high power diode lasers have previously been developed is the near infrared from 0.7 to 2.4 μm.[2,3] These lasers are based upon the use of gallium arsenide technology and have been developed primarily for the telecommunications industry for fibre optic communications. They are therefore technologically very advanced because of their widespread use, whereas the lead salt devices are mainly used for spectroscopy, and hence there had been far less technological push to produce efficient lasers for the longer wavelength infrared region.

The design and fabrication of the first QC lasers in the Capasso group[4] at the Lucent laboratories in Murray Hill has allowed mid infrared lasers to be developed based upon gallium arsenide and similar technologies developed for optical communications. Hence the variety of growth methods developed for the telecommunications lasers could be applied to a new way of generating infrared light. In particular, methods such as molecular beam epitaxy (MBE) had been developed for depositing very thin layers of semiconductors for semiconductor device manufacture.

The QC laser relies upon the generation of a type of artificial semiconductor based upon the use of alternating lasers of different types of semiconductor materials. This can produce sets of square well potentials. The wavelength of the emitted light is then dependent upon the properties of the square wells, rather than the band gap of the initial material. Although the original idea for this type of laser was proposed by Kazarinov and Suris[5] in 1971, it was not until semiconductor device technology had become mature that the design, fabrication and operation of a QC laser was described by Faist *et al.*[4] in 1994.

In the QC laser the light is generated by a transition between energy levels in a square well based potential. The scheme used in the first QC lasers is shown in Fig. 1. It is essentially a three level laser. Electrons are injected *via* an injector miniband into level 3, light is emitted by a transition from level 3 to level 2. Rapid relaxation then takes place from level 2 to level 1, which is then coupled into the injector miniband which populates the upper level in the next stage of the cascade. Fig. 1 also contains a duplication of the basic lasing unit as an example of a small section of an arrangement of multiple quantum wells. The effect of an applied electric field is to cause the cascade structure shown. The detailed calculations of the ''band-gap engineering'' necessary and the subsequent realisation of this in a practical device were carried out in Capasso's group at Lucent Technologies.[4] The original laser structure, designed to operate at 4.26 μm, was grown by using molecular beam epitaxy, in which up to 25 identical stages of active region and electron injector were grown. The quantum well layers consisted of $Ga_{0.38}In_{0.62}As$ and barrier layers of $Al_{0.6}In_{0.4}As$. The energy level spacing of the laser transition was $E_3-E_2 = 295$ meV, and the separation between the lower level of the laser transition to the relaxation level $E_2-E_1 = 30$ meV.

QC lasers have much higher output powers than lead salt lasers and have very narrow linewidths. Since the gain profile

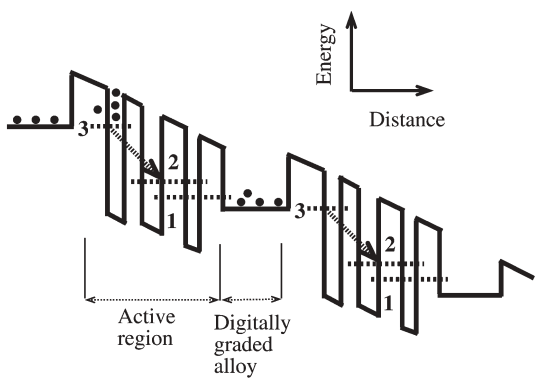

Fig. 1 A schematic conduction band energy diagram of a portion of a section of a quantum cascade laser. Electrons are injected through a barrier into the $n = 3$ energy level of the active region. The laser transition takes place between levels 3 and 2. The lower state is depleted by coupling to level 1 of the adjacent well. They then are transferred to the next injection region of the cascaded structure and the process is repeated. (After Faist *et al.*, Ref. 4.)

of a unipolar QC laser is approximately symmetric, their intrinsic line width is predicted to be much narrower than that of a bipolar diode laser operating in the same spectral region.[4] This has led to the possibility of carrying out a wide variety of experiments which require narrow linewidth, tunability and high power such as sub-Doppler saturation spectroscopy, or sensitive detection of the composition of the earth's atmosphere.

At present most spectrometers use distributed feedback (DFB) single mode QC lasers which operate either continuously at liquid nitrogen temperature, 77 K, or in pulsed mode at room temperature. Some QC lasers have been operated continuously at room temperature for short periods of time,[6,7] but are not currently commercially available for installation into spectrometers.

The tuning mechanism of semiconductor lasers depends upon the variation of the index of refraction of the laser with temperature and with current. In lead salt lasers there is a specific contribution to the current tuning associated with the number of free charge carriers, electrons or holes, resulting in a carrier dependent index of refraction, as well as that associated with temperature. The tuning mechanism of distributed feedback (DFB) QC lasers is very different from that of lead salt lasers since it depends upon the temperature tuning of the refractive index of the waveguide which changes the apparent optical length of the wavelength selection grating. This change may be slow, if the temperature of the laser structure is varied using a Peltier device, or very rapidly if caused by the resistive Joule heating within an electrical current pulse. A sweeping of a laser frequency is referred to as a frequency chirp.

Experiments carried out by Faist *et al.*[8] showed that the laser frequency swept rapidly to lower frequency during a current pulse (a frequency down-chirp) but that it maintained a very narrow instantaneous line width as its frequency chirps as expected from the calculated behaviour of a QC laser. They also demonstrated that in these first generation lasers the temperature rise of the active region during a 100 ns current pulse could be up to 20 °C, causing a rapid change of the index of refraction of the "bulk constituent materials".

Most of the spectrometers based upon the use of quantum cascade lasers comprise a QC laser driven by a specific type of drive control system, a long path length multiple pass absorption cell, and a cooled infrared detector attached to an appropriate detection system. This is shown schematically in Fig. 2. The high output power of the QC laser means that very long absorption paths may be used, typically from about thirty to two hundred metres. Most of the multiple pass cells are based upon a variant of the Herriott cell.[9] The design of spectrometers which have been developed to use continuously operating QC lasers is very similar to those which use lead salt lasers. The QC lasers are housed in liquid nitrogen cooled Dewars and scanned using a current ramp. One of the first systems of this type was developed by Sharpe *et al.* at PNNL.[10] In some experiments, such as those of Webster *et al.*[11] the laser is housed within an existing lead salt spectrometer system such as the airborne ALIAS instrument. An example of a typical absorption spectrum of nitrous oxide recorded using the PNNL[10] QC laser spectrometer is shown in Fig. 3. At the low gas pressure in the astigmatic Herriott absorption cell the

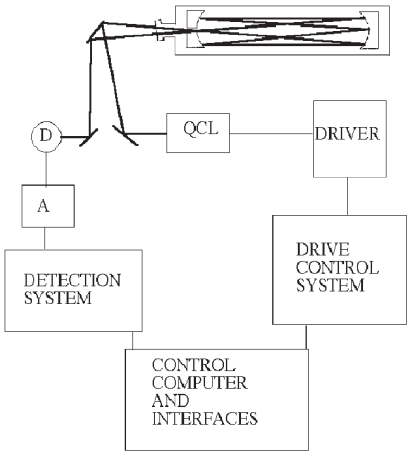

Fig. 2 A schematic diagram of a typical experimental arrangement of a quantum cascade laser spectrometer.

sub-Doppler linewidth of the lasers leads to the recording of a Doppler limited spectrum.

For room temperature operation pulsed lasers are used. Two particular types of instrument have been developed, the inter-pulse[12–14] and the intra-pulse spectrometer.[15,16] In the first type, the inter-pulse spectrometer, an attempt is made to limit the frequency chirp within a current pulse by using very short pulses, so that a narrow chirp-limited line width is obtained. This line is then swept over a known frequency range by applying a sub-threshold current ramp to the laser. Using this method a single narrow frequency interval is recorded for each current value of the sub-threshold ramp. The resultant spectrum resembles that produced by a typical current swept lead salt laser spectrometer, but one having a broader effective linewidth. The first system of this type was demonstrated by Namjou *et al.*,[12] and used additional modulation for phase sensitive detection of the absorption. Most of the subsequent

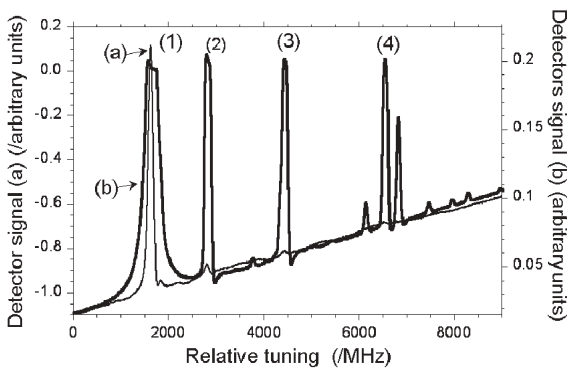

Fig. 3 Examples of the spectra of nitrous oxide obtained using the EMSL QC laser spectrometer at PNNL,[11] scanning from low to higher frequency. (a) Short 10 cm cell, pressure 0.4 Torr N_2O (b) Astigmatic Herriott cell, 100 m pathlength, pressure 20 mTorr N_2O. The transitions identified are (1) P34, 00^01–00^00 band, $^{14}N^{14}N^{16}O$, 1254.47269 cm^{-1}; (2) P41, 01^11–01^10 f band, $^{14}N^{14}N^{16}O$, 1254.51180 cm^{-1}; (3) P29, t 00^01–00^00 band, $^{14}N^{15}N^{16}O$, 1254.56517 cm^{-1}; and (4) R9, 00^01–00^00 band, $^{14}N^{14}N^{18}O$, 1254.63426 cm^{-1}. The reduction of laser power during the scan causes the baseline variation.

development of the inter-pulse spectrometer by the groups at Rice University[13] and Aerodyne[14] has used sweep integration combined with pulse normalisation, rather than phase sensitive detection. A typical spectrum is shown in Fig. 4.

In the intra-pulse spectrometer[15] a long current pulse is used so that the laser frequency sweeps to lower frequency during the pulse, a frequency down-chirp. A complete spectrum of a frequency micro-window is then recorded during each pulse. This method requires a very wide frequency bandwidth infrared detector and amplifier combination, and also a fast and efficient digitiser. In Fig. 5(a). we show an example of a typical laser pulse used in an intra-pulse spectrometer. The trapezoidal shape is typical of that produced by an efficient QC laser. The non-linear tuning is shown by the increase in the separation of the Ge etalon fringes with increasing time. This results from an effective temperature rise of 20 °C during the current pulse. The signal obtained when a low pressure of nitrous oxide is introduced into the cell shows strong, sharp asymmetric absorption lines. The background of this signal and that of the empty cell superimpose exactly. A single mode tuning range of *ca.* 3 cm^{-1} may be seen.

The resolution limitations of both the short pulse and the frequency down-chirp methods are similar, and are set by the transform limit of the pulse,[13,14] or of the bandwidth–time duration product of the signal detected by the fast detection system.[15]

In their assessment of the resolution limitations of their short-pulse spectrometer, Kosterev and his colleagues[13] showed that about 75% of the laser energy lies in the transform-limited part of the spectrum. By analysing the line shapes of their spectra they have demonstrated that a full width at half maximum (FWHM) of 9.5 × 10^{-3} cm^{-1} (290 MHz) may be achieved. They have also shown that care is needed to lessen the effects of energy in the tail of the laser pulse. Nelson and his colleagues[14] have concentrated on reducing the effective line width (FWHM) of a pulsed laser to 7.4 × 10^{-3} cm^{-1} by running the laser close to its threshold current and eliminating the pulse tail. In Fig. 4 an example is shown

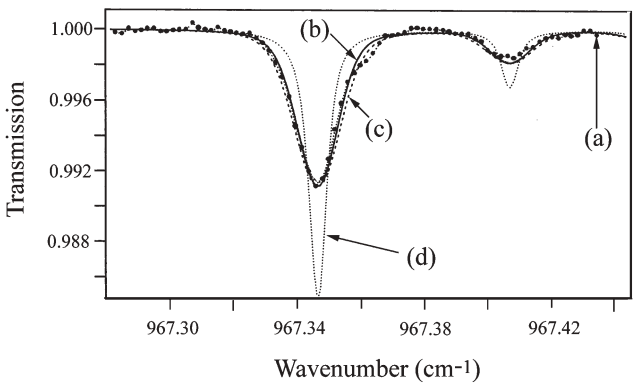

Fig. 4 An example of an absorption line of the spectrum of ammonia recorded using the Aerodyne inter-pulse spectrometer. (a) Data, tdl fit: 22ppb, line width (half width half height) = 0.006 cm^{-1}, (b) HITRAN simulation, 22.3 ppb NH_3, (c) simulation convolved with a Gaussian laser linewidth of 0.0059 cm^{-1}, and (d) best simulation with a line width of 0.007 cm^{-1}, 25 ppb. (Reproduced by permission of M. S. Zahniser, Aerodyne Research Inc.)

of the way in which they have analysed the effective line width and shape of their spectrometer using absorption lines of ammonia.

The resolution of the intra-pulse spectrometer is not determined by the effective line width of the laser induced by the current pulse, but by the chirp rate of the laser and the temporal resolution of the detection system. In both the short pulse and in the frequency down-chirp spectrometers, the bandwidth-duration product of a signal cannot be less than a certain minimum value, the "uncertainty relation". This relationship is described in detail by Bracewell,[17] who has given the proof that the product of the equivalent duration, Δt, and the equivalent bandwidth, Δv, must exceed or be equal to $C = (4\pi)^{-1}$. For a rectangular time window $\Delta t \Delta \nu \geqslant C = 0.886$, and for a Gaussian window $\Delta t \Delta \nu \geqslant C = 0.441$. In the description of their short pulse spectrometer Kosterev *et al.*[13] have shown that their resolution of 290 MHz cannot be significantly improved by changing the pulse length. If the pulse were to be shortened there would be a Fourier transform limitation of the resolution, whereas if it were lengthened the frequency chirp would be excessive. A similar analysis may be carried out for the limitations of the time resolved detection system,[15] as was first shown for a pulsed lead salt laser by Gorshunov *et al.*,[18] and in more detail by McCulloch *et al.*[15] This gives a chirp rate limited resolution of $\Delta v = \sqrt{C \mathrm{d}v/\mathrm{d}t}$. In the limiting case of $C = 1$, and a rapid frequency chirp rate of 200 MHz ns^{-1} which is characteristic of some pulsed QC lasers, the limit of resolution would be 447 MHz, (or 0.015 cm^{-1}). If the chirp rate is reduced to 20 MHz ns^{-1}, and if a rectangular window function is used, this resolution limit would fall to 133 MHz, (or 0.0044 cm^{-1}). The chirp rate and resolution calculated for the N_2O spectrum of Fig. 5(a) are shown in Fig. 5(b).

When very low pressure samples of pure gases are studied, the high resolution QC laser spectrum of Fig. 5(a) also demonstrates that the instrument line shape of the intra-pulse spectrometer has a characteristic hook shape. This line shape resembles that of the original swept field NMR or ESR spectrometers and is due to rapid passage. A more complete description of its analysis will be given in the section devoted to non-linear spectroscopy.

Trace gas detection and analysis

One of the main uses of cryogenically cooled lead salt lasers has been for atmospheric sensing. Their applications have ranged from the observation of stratospheric molecules associated with the ozone layer, to the detection in the boundary layer, or lower troposphere, of methane fluxes from peat bogs and to measurements of air pollution in cities. Most of these spectrometers use a layout similar to that shown in Fig. 3, with a long pathlength absorption cell such as an astigmatic Herriott cell, and a laser cooled to 77 K. The laser frequency is usually swept over a narrow wavenumber window of up to about 0.4 cm^{-1} within which the strong target lines of the gases may be measured. For use in the lower atmosphere the pressure in the long pathlength cell is often reduced to that of a tenth of an atmosphere or less. Although this reduces the number density of the trace molecules it enhances their detectivity since it reduced the pressure broadening of the

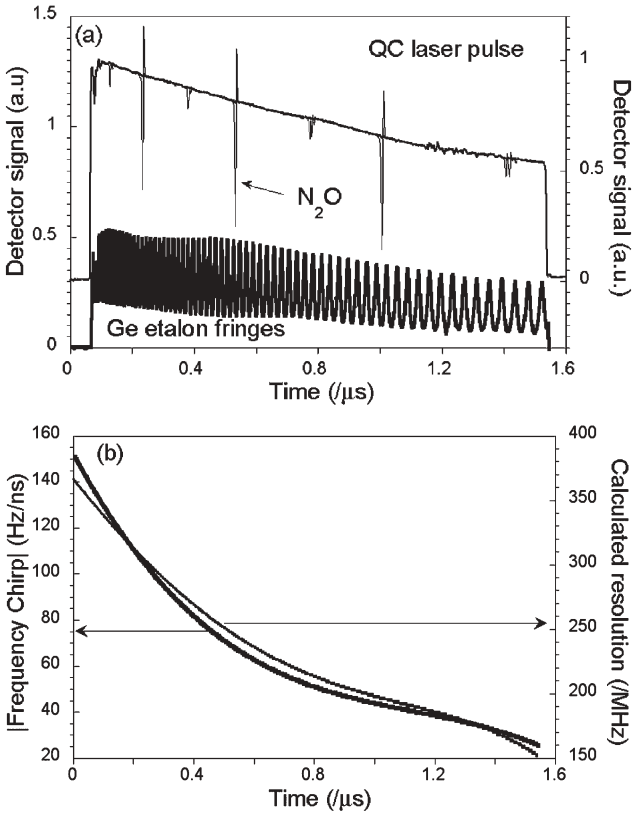

Fig. 5 (a) Time dependence of a QC laser pulse of 1.5 μs duration passing through a 100 m pathlength astigmatic Herriott cell; heavy line, empty cell; light line, *ca.* 1 mTorr N_2O. The fringes produced using a Ge etalon with 0.048 cm^{-1}–free spectral range are displaced for clarity. The scan window is *ca.* 3 cm^{-1}. (b) The calculated chirp rate (MHz ns^{-1}) and resolution (cm^{-1}), assuming a rectangular window function, of the QC laser spectrum shown in Fig. 5(a).

lines and hence their overlap. The use of a reduced pressure therefore allows much better resolution of closely spaced lines and also background discrimination. In the upper troposphere and stratosphere the atmospheric pressure is sufficiently reduced from that at ground level that the principal source of line broadening is the Doppler effect.

Some of the first uses of QC lasers in *in-situ* atmospheric sensing have been as drop-in replacements for lead salt lasers. A good example of this is their use in the ALIAS instrument of the Webster group[11] for stratospheric measurements of the concentrations of nitrous oxide and of methane. The main modification made to the spectrometer was to use an addition power supply matched to the QC laser, and to mount the QC laser on a package to allow it to fit into one of the four positions usually occupied by a lead salt laser. An example of their simultaneous measurements of the spectra of nitrous oxide and methane is shown in Fig. 6. They were also able to carry out an inter-comparison of the amounts of methane measured using both the QC and lead salt lasers. As a result of this inter-comparison Webster and his colleagues concluded that "the single mode QC laser, cooled to 83 K, produced higher output power (10 mW), narrower laser linewidth (17 MHz) and better spectra stability ($\sim$0.1 cm^{-1} K^{-1})" than the comparison lead salt laser. Based on this result they

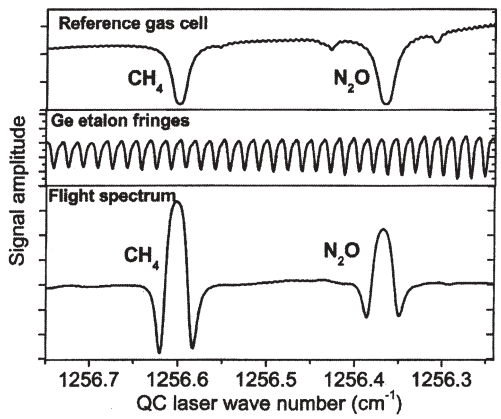

Fig. 6 QC laser spectral scans of a reference gas cell 5 cm long, a Ge etalon with a free spectral range of 0.015 cm^{-1} and a flight spectrum of the ALIAS spectrometer showing second-harmonic line shapes from CH_4 and N_2O. The laser wavelengths are scanned with a current ramp and a superimposed sinusoidal modulation for second harmonic detection. The scanning ramp frequency is 10 Hz and individual scans co-added to produce a 1.3 s spectral average. Four spectra such as this are recorded in-flight each 1.3 s, produced in 80 passes of the 1 m long multipass cell of ALIAS. During flight the cell is kept at a constant temperature of 280 K. (Reproduced with permission of the Optical Society of America from Ref. 12.)

estimated that their measurement precision was increased over that of the lead salt lasers by a factor of 3, leading to a minimum detectable concentration of methane of approximately 2 parts per billion by volume.

The sensitivity of the QC laser based ALIAS spectrometer is demonstrated by the detection of the minor isotopic components of water in the recent spectrum shown in Fig. 7. This has allowed the JPL group to shed some light on the source of the water found in the stratosphere, since the isotopic depletion observed points to two possible mechanisms for dehydration of the upper troposphere, convective dehydration and gradual dehydration. Owing to the coupling between the upper troposphere and lower stratosphere, this also gives information

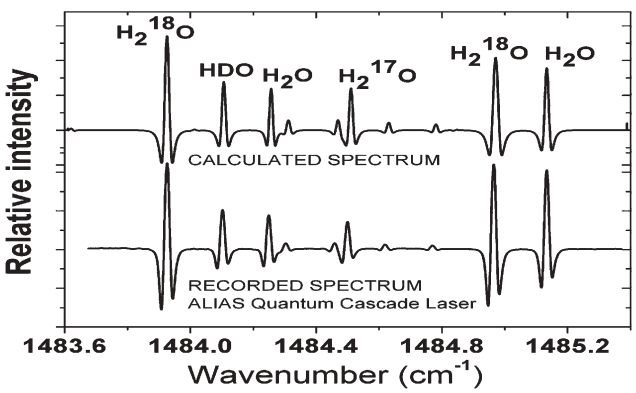

Fig. 7 QC laser spectra of water in the upper troposphere recorded using the ALIAS spectrometer. The region is chosen so that the isotopomers are easily identifiable. Their relative concentrations are used as inputs for modelling of the dehydration of the upper troposphere. (Reproduced by permission of C. R Webster of the Jet Propulsion Laboratory.)

about the water content of the stratosphere. The processes which may lead to this type of variation have been discussed in some detail by Webster and Heymsfield[19] and by Rosenlof.[20]

The developments of instruments for sampling the concentrations of trace molecules in the lower troposphere and boundary layer has followed a similar path to that chosen for the upper atmosphere. However unlike the stratospheric instruments, the majority of the spectrometers currently being developed and used are based upon the use of pulsed QC lasers, since it allows the lasers to be cooled electrically *via* Peltier coolers, eliminating the need for a bulky liquid nitrogen Dewar.

The first QC laser based systems to be both developed and deployed were those of the Rice University[13] and Aerodyne groups.[14] Both used the inter-pulse method using a short duration current pulse, with the tuning being provided by a sub-threshold current ramp. Since the sub-threshold current tuning method does not lend itself to long wavenumber scans, instruments developed to measure two or more species usually use two or more diodes, often one for each micro-window region used to detect a particular atmospheric constituent. Perhaps the most complex instrument of this type is the inter-pulse spectrometer developed by the Aerodyne group of Nelson, McManus and Zahniser.[21] This instrument may be used with up to four QC lasers simultaneously, leading to the use of a complex pulse delay method to allow the spectra for all four lasers to be collected sequentially. Examples of four simultaneously recorded spectra are shown in Fig. 8. A similar but more compact instrument has also been used for monitoring two closely spaced lines of methane and nitrous oxide.[22] The determination of the ratio of the concentrations of nitrous oxide and methane is a key factor in studies of atmospheric structure and of chemical transport. Their latest results, shown in Fig. 9, may be compared with those obtained with the ALIAS instrument by the Webster group,[11] Fig. 6, using an alternative pair of closely spaced lines. In these recent experiments by the Aerodyne group, in which the concentrations of nitrous oxide and methane were measured, the liquid nitrogen cooled mercury cadmium telluride detector was successfully replaced by one which was thermoelectrically cooled. This will allow future field versions to be operated without the need for cryogens, making unattended operation a possibility.

In the alternative method of using pulsed QC lasers, the intra-pulse method,[15,16] most of the developments so far have

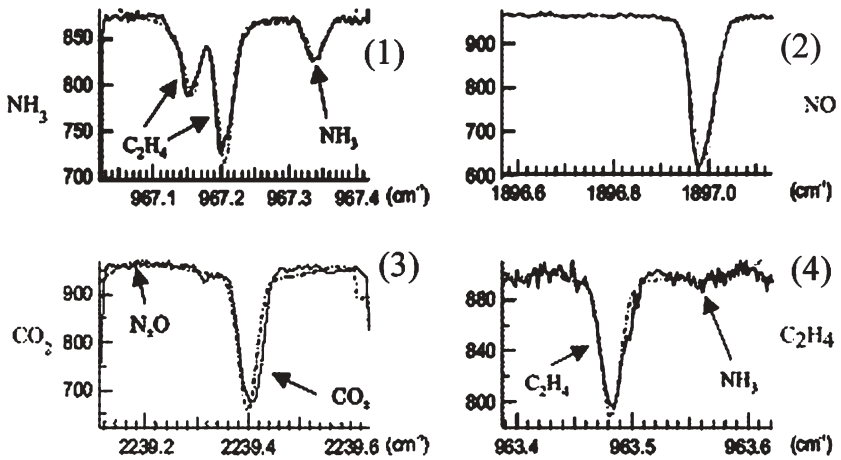

Fig. 8 Spectra collected from the four laser version of the Aerodyne inter-pulse QC spectrometer. Laser 1, fitting to NH_3 and C_2H_4, laser 2 fitting to NO, laser 3 fitting to CO_2 and N_2O, and laser 4 fitting to C_2H_4 and NH_3. (Reproduced from Ref. 23 with permission of Elsevier.)

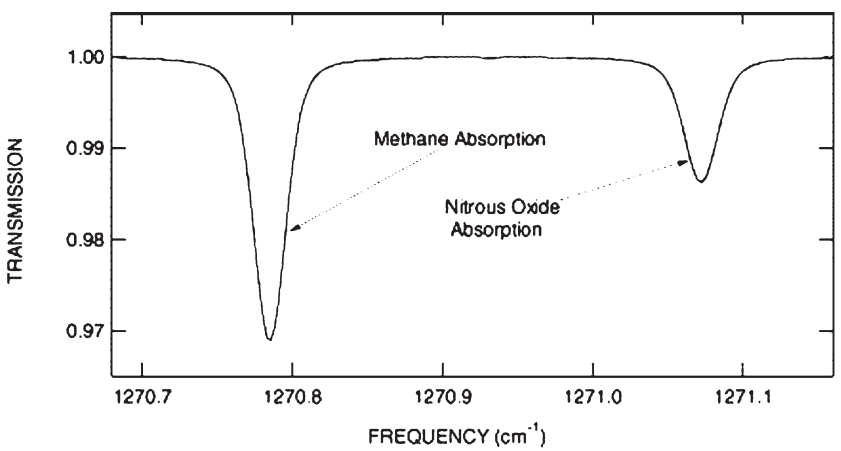

Fig. 9 Simultaneous monitoring of N_2O and CH_4 in ambient air with a single TE cooled QC laser and a TE cooled infrared detector from Vigo Systems Ltd. (Reproduced from Ref. 24 with permission of Elsevier.)

been carried out by the Strathclyde University group of Duxbury and Langford.[15] A recent example has been the study of the spectra of the exhaust gases of automobiles by McCulloch *et al.*[23] In this series of experiments the QC laser operated at 10.24 μm, and the variation of the concentrations of ethylene and carbon dioxide in a variety of vehicle exhausts was investigated.

Since the intra-pulse method involves the use a long duration current pulse, it is most successful with lasers which have a low current threshold. By switching from the 10 μm to the 8 μm region we can exploit the excellent low current threshold of the 8 μm QC lasers. As a result longer duration current pulses may be used than in the 10 micron region, and longer wavenumber regions can be scanned during a single pulse. In order to compare the results of an intra-pulse spectrometer with those from the other systems described above we will concentrate on measurements made in the 8 μm region. In Fig. 10. we show a spectrum of the ambient atmosphere recorded using a current pulse of 1.3 microseconds duration (Fig. 10a), and an expanded portion of the central part of a spectrum (Fig. 10b). Within this micro window two closely spaced lines of nitrous oxide and methane may be seen. Although the average concentration of methane is *ca.* 1.7 ppm whereas that of nitrous oxide is *ca.* 0.3 ppm, by a coincidence the relative absorption cross sections of these particular absorption lines are such that at ambient concentrations of these gases these lines should appear to have very similar intensities. Since the concentration of nitrous oxide is slowly varying, the changes of the relative intensities shown in this figure demonstrate the fluctuations in the concentration of methane and water in the neighbourhood of the Physics Department of Strathclyde University compared to that within the QC laser laboratory.

In order to demonstrate that this type of instrument may be used to detect a wide range of gases within this particular micro window, in Fig. 11. we show two spectra of breath, and in Fig. 12 the spectra of samples of cigarette smoke. The detection of the variation of the concentrations of methane, water and carbon dioxide in the samples of breath, Fig. 11, shows that the wide tuning range of the intra-pulse spectrometer allows the simultaneous recording of the spectra of molecules with very different line densities. The high quality of the spectra of the cigarette smoke in Fig. 12 shows that the laser has sufficient intensity to penetrate a highly scattering atmosphere, so that a very long path length in the multiple pass cell may still be used. It also demonstrates that the main effect of particulates is to change the background level of the spectrum, which may be compensated for providing that the resolution is sufficient to allow the background level to be determined. Although cigarette smoke contains a very wide range of combustion products most are too large or too involatile to yield resolvable gas phase spectra. The main chemical signature which occurs in the spectrum of cigarette smoke, but not in the spectra of the atmosphere or of automobiles which we have also recorded, is formaldehyde,

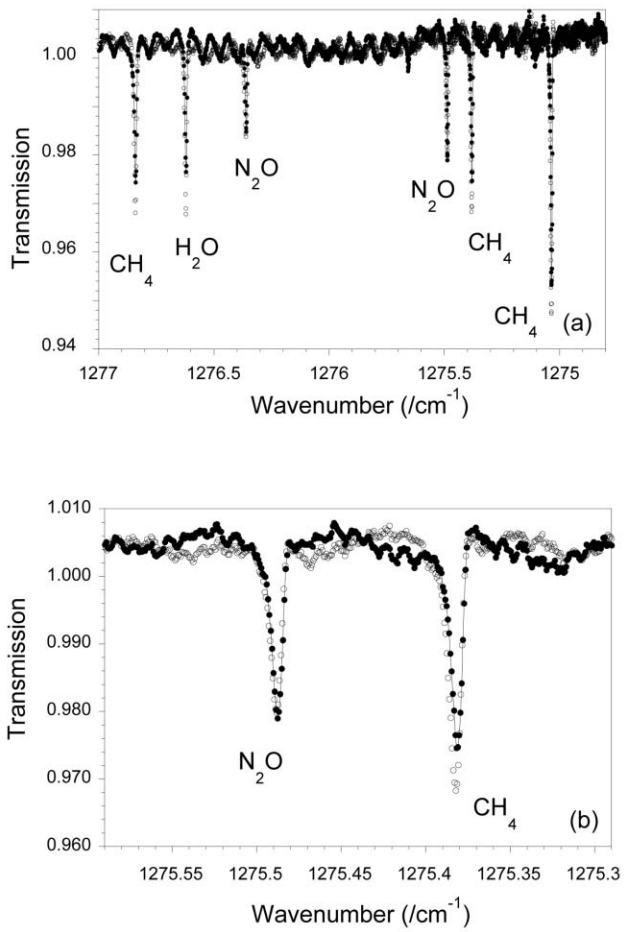

Fig. 10 Expanded mid pulse sections of two long intra-pulse scans of atmospheric samples, path length 100 m, pressure 15 Torr. The integrated absorption coefficients of these lines of CH_4 and N_2O are almost inversely proportional to their average atmospheric abundances, so that their relative intensities should be almost equal. The variation between the spectrum of the atmosphere on the building roof -●-, and within the laboratory -○-, probably reflect variations in the methane concentration, since the intensity of the nitrous oxide line remains constant.

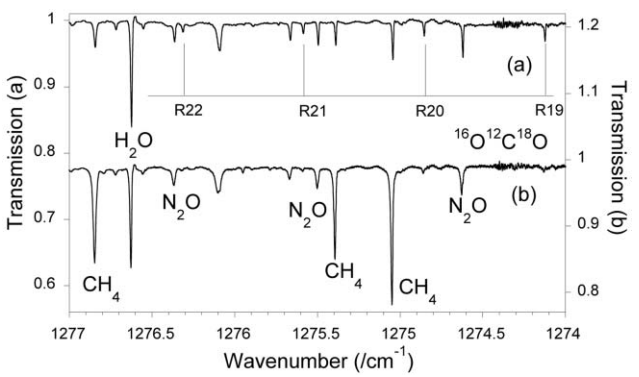

Fig. 11 Examples of the intra-pulse spectra of the breath two different volunteers recorded using a pulse duration of 1.27 microseconds, and a pulse repetition frequency of 20 kHz averaged for one second. The absorption path length was 100 m and the cell pressure 15 Torr. (a) Efficient production of carbon dioxide detected *via* the very weakly allowed 8 μm band of the unsymmetrical isotopomer $^{16}O^{12}C^{18}O$, small methane output. (b) A very small signal from carbon dioxide but a large methane output. Both (a) and (b) have approximately the same output of water.

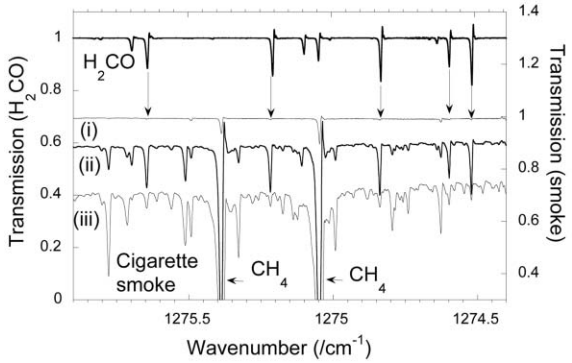

Fig. 12 A comparison of the spectrum of formaldehyde (H_2CO) with that of cigarette smoke. The path length and sample number are identical to those used for Fig. 11. After evacuation the cell "smoked" the cigarette for a period of up to 20 seconds. This process was then repeated. (i) beginning of puff 1, strong CH_4 absorption, (ii) late in puff 1, strong H_2CO absorption, (iii) puff (1) max., H_2CO reduced, CH_4 increased, a complicated spectrum of other minor constituents is also seen. The change in the position of the baseline from (i) to (iii) shows the effect of the scattering due to the particulates in the smoke.

which possesses a rich, strong, and well resolved spectral fingerprint within this particular micro window.

Some of the most difficult molecules to detect in the atmosphere are free radicals. A recent experiment by Ganser *et al.*[24] making use of the Faraday rotation detection method has been used to detect low amounts of the stable free radical NO. This demonstrates that the combination of a QC laser spectrometer with Faraday modulation methods may be a powerful tool for the future detection of atmospheric free radicals.

Spectroscopic applications of the power, narrow linewidth and time dependent properties of quantum cascade lasers

Introduction. In the period when tunable lead salt diode laser spectrometers were being developed[1,2] from 1970 to 1980 there was great interest in the possibility of using the high power of laser sources for exploring a variety of types of non-linear spectroscopy. Since the lead salt lasers were inherently low power, most of the experiments were based upon the use of continuously operating high power line tunable carbon dioxide and carbon monoxide lasers.[2] As these lasers have a very limited tuning range on a single vibration–rotation line, the transitions between the molecular energy levels were usually tuned into resonance with the laser by using electric or magnetic fields, laser Stark and laser magnetic resonance spectroscopy.[2] Another method used used somewhat later was to add microwave sidebands to a fixed frequency laser, giving considerable tunability but low output power.[2,3]

At low gas pressures the main source of line broadening in infrared spectra is the Doppler effect.[2,3] The absorption frequency of the laser radiation is higher than the centre frequency if a molecule is moving parallel to the direction of propagation of the laser beam and lower if antiparallel. This results in an inhomogeneously broadened line and is shown schematically in Fig. 13(a). A high power laser interacting with a low pressure gas may therefore pump molecules from the lower energy level to the higher energy level of the transition, reducing the population difference and creating a population "hole". Using the high power and narrow linewidth of molecular gas lasers a variety of experiments were carried out on sub-Doppler hole burning spectroscopy.[3] These allowed the selection of a narrow velocity group of molecules around line centre of a Doppler broadened line, Lamb dip saturation spectroscopy, and a variety of double resonance experiments such as optical–optical double resonance (OODR) in which two or more frequencies are used to interrogate the molecular sample.[2] The creation of the Lamb dip caused by the double interaction of the forward and backward running waves with the same zero velocity group of molecules at line centre, Fig. 13 (b), (see also Ref. 2).

Not only were time independent processes studied, but a variety of transient phenomena were studied by rapidly switching transitions into resonance with fixed frequency carbon dioxide lasers using pulsed electric field tuning. Many of these experiments were carried out at the IBM research laboratories by Brewer's group,[25] and also by Loy.[26] To understand the resultant signals, each molecular absorption line studied was treated as a transition between two isolated energy levels, a two level system. The population difference between the upper and lower levels, and also the electric field driving transitions between the levels, is time dependent. The behaviour of the output signal from a group of molecules, in which this transition is excited, is then dependent upon the

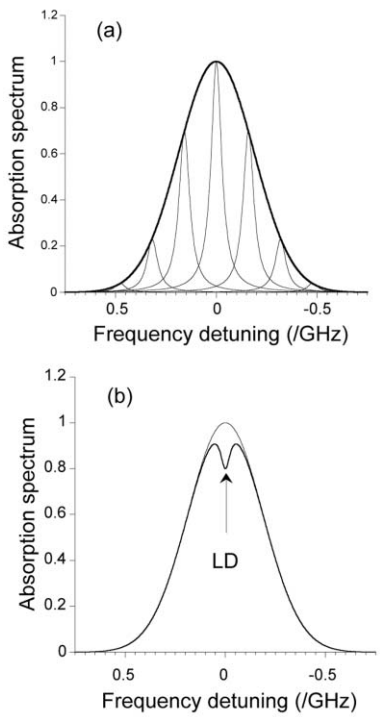

Fig. 13 The structure and saturation of a molecular Doppler broadened absorption line. (a) A schematic diagram of the contributions of the contribution of the separate Doppler shifted homogeneously broadened components to produce an inhomogeneously (Doppler) broadened line. (b) The appearance of a narrow saturation feature (Lamb dip, LD) at line centre when the molecule is subjected to a standing wave field (see Ref. 2).

duration of the pulse, the power of the laser, the rate of change of frequency during the pulse, and the relaxation processes due to molecular collisions. Although in a review article written in 1978 Shoemaker[27] suggested that it would be interesting to generalise the experiments by using tuneable lasers, at that time it was believed that diode lasers of the necessary power were unlikely to become available.

Since the single mode output power of a QC laser is higher than that of a lead salt laser by a factor of a hundred or greater, it is now possible to envisage carrying out both time-independent and time-dependent studies of the behaviour of molecular transitions subjected to strong electromagnetic radiation fields by using tuneable high power infrared lasers, both continuous and pulsed.

Saturation spectroscopy using continuous QC lasers

The first experiments of this type which were carried out were demonstrations of the possibility of detecting narrow saturation dips using continuously operating QC lasers. Although there has been one clear demonstration of Lamb dip spectroscopy using a lead salt diode laser by Murtz *et al.*,[28] this required a complicated experimental realisation in which the laser was frequency offset-locked to a CO laser. The good free running stability and high power of cw DFB QC lasers has opened up the possibility of carrying out non-linear or hole burning experiments with sub-Doppler resolution using free running QC lasers. The first demonstration of this was by Remillard *et al.*,[29] who observed sub-Doppler resolution limited Lamb dip signals in transitions in NO using a 5.2 micron DFB QC laser. In order to use a double pass through a 20 cm path length cell a tilted wire grid polariser was used to reduce the feedback into the laser. The main limitation in their resolution of *ca*. 4.3 MHz full width at half maximum height was due to frequency fluctuations associated with the stability of the laser power supply. More recently Kelly and his colleagues[30] have analysed in some detail the effects of electrical noise in the laser power supply, and also their ability to detect unidirectional hole burning signals in both nitric oxide and methyl iodide.

In a further series of measurements at PNNL by Taubman and his colleagues[31] cavity enhanced absorption spectroscopy has been employed. In the simplest implemention the QC laser is locked to a high finesse optical cavity which contains the gas to be studied. The laser radiation is coupled into the cavity *via* an acousto-optic modulator and a Faraday isolator to minimise back reflections into the laser. The spectrum is obtained by scanning the optical cavity length, and hence the frequency of the laser which is locked to the cavity. Examples of the narrow lamb dips obtained in this way are shown in Fig. 14. The group then showed that if the more complicated modulation scheme developed by Ye *et al.*,[32] Noise immune Cavity Enhanced Optical Heterodyne Molecular Spectroscopy, (NICE OHMS), is used, very high resolution low noise spectra can be obtained. This method adds to the direct absorption method the use of frequency modulation and phase sensitive detection, and also resonant sideband modulation. Spectra using the NICE OHMS methods are shown in Fig. 15. In Fig. 15 (a) and 15 (b) the NICE OHMS spectra are

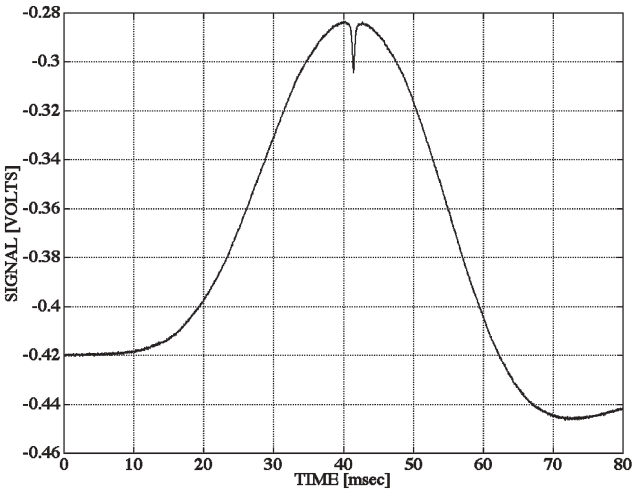

Fig. 14 Cavity enhanced absorption feature in nitrous oxide at 5.33 Pa (40 mTorr) showing the Lamb dip at the peak of a Doppler broadened line. The empty cavity finesse was 11770 and the intra-cavity saturation approximately 10. Absorption increases in the upward direction in this figure. (Reproduced from Ref. 33 with permission of Elsevier.)

compared with Lamb dip spectra with (a) and without (b) a good lock to the optical cavity. It can be seen that the NICE OHMS signal shows better immunity from the effects of a poor optical cavity lock.

Non-linear optics and coherent population transfer

Not only have the lasers sufficient power to carry out saturation spectroscopy, they may also be swept in frequency very rapidly by applying a current pulse. This allows QC lasers to be used to carry out efficient rapid passage experiments of the type pioneered by Brewer[25,27] and Loy[26] on molecular gases. This type of experiment may also lead to an efficient way of coherently inducing population transfer between vibration–rotation states, which is often the first step in the production of quantum control of processes.

In the course of developing an intra-pulse spectrometer using a long pathlength astigmatic Herriott cell for trace gas sensing,[15,23] McCulloch *et al.*[33] discovered that they were observing very unusual line shapes in the spectra of low pressure gases. In these spectra each absorption line appeared to be followed by an emission spike. Some of the cleanest examples of this type unusual line shape were found when studying the vibration–rotation lines of the ν_3 band of nitrous oxide as shown earlier in Fig. 5(a).

In Fig. 16 a transmission spectrum of a low pressure sample of nitrous oxide is shown which covers most of the spectral region of Fig. 5(a). In the inset in this figure the change in shape of the P(12) line is shown as a function of the addition of increasing amounts of nitrogen. As the nitrogen is added the ''emission '' signal is gradually quenched, and above a critical pressure of about 25 Torr a ''normal'' pressure broadened line shape is regained. The pressure broadened halfwidth at half height of this line at a pressure of 25 Torr has been measured to be *ca*. 160 MHz, a mean time between collisions of 6.25 ns, whereas at the starting pressure of *ca*. 25 mTorr the mean time

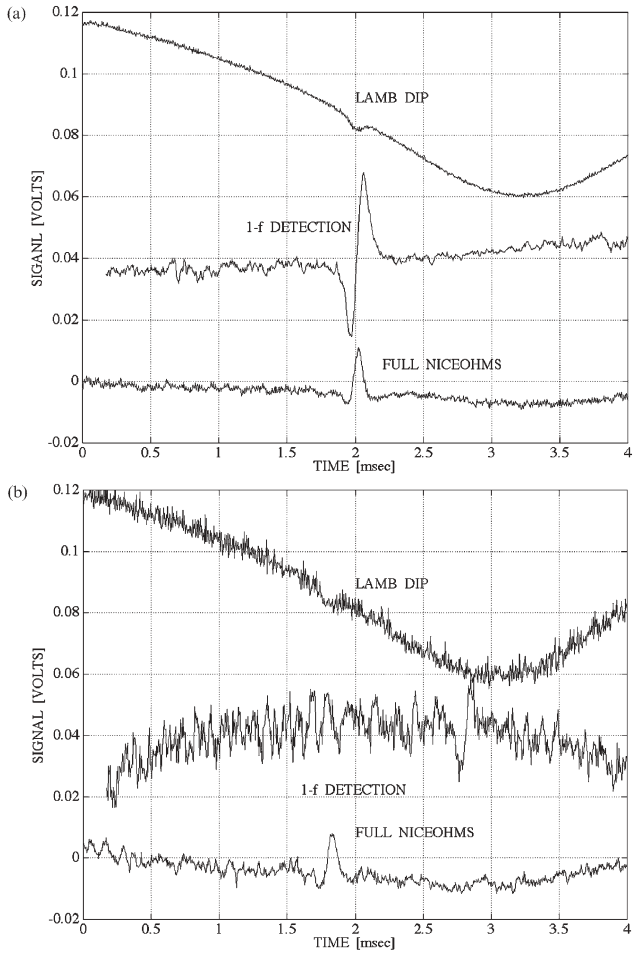

Fig. 15 (a) Traces showing the Lamb dip using direct cavity transmission, 1f recovery, and full NICE-OHMS. The NICE-OHMS trace has a symmetric shape rather than the dispersion shape of the 1f signal due to the extra order of demodulation. (b) These are the same as the traces as shown in (a) except that the lock between the QCL and the optical cavity was deliberately degraded. The direct absorption and the 1f recovery traces are degraded more than the NICE-OHMS trace, which is only marginally affected. (Reproduced from Ref. 33 with permission of Elsevier.)

between collisions is *ca*. 6 μs, which is much longer than the duration of a laser pulse. This shows that in the low pressure spectra of the pure gas collisional energy transfer and collisional dephasing of the transition dipole moment play a very minor role.

It is possible to vary the rate of chirp of a QC laser through an absorption line by placing it in different positions under the chirp envelope of a laser. This can be achieved by modifying the starting frequency of the laser and by adjusting the temperature of the laser substrate. The number density of the molecules being probed may be adjusted by changing the gas pressure in the long pathlength absorption cell. It was found that the line shape of a pure gas depends upon the chirp rate, the transition dipole moment, and the number density of the nitrous oxide.

In Fig. 17 the change in structure and resolution of two types of transition in nitrous oxide are shown when the chirp rate is reduced by approximately a factor of 8 from 161 MHz ns^{-1} to

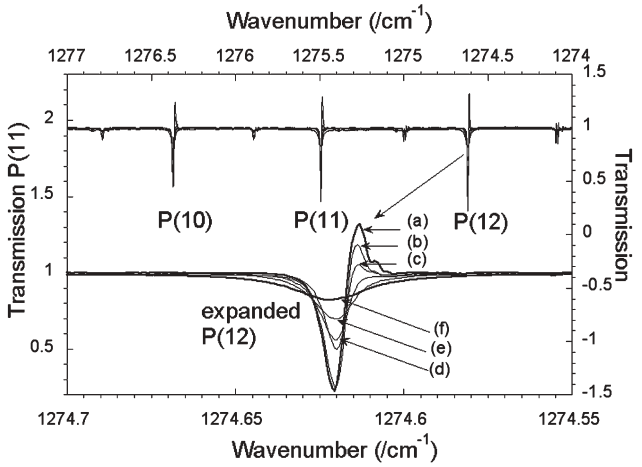

Fig. 16 A low pressure intra-pulse transmission spectrum of nitrous oxide recorded using a laser pulse duration of 1.27 microseconds and a pulse repetition frequency of 20 kHz averaged for one second. The path length was 110 m. The main vibration–rotation lines of the ν_3 band of nitrous oxide is indicated. (a) is the spectrum of 0.005 Torr of pure gas. In the spectra (b) to (f) nitrogen was added as a buffer gas to a total pressure of (b) 4.6, (c) 12.3, (d) 25.3, (e) 50.1 and (f) 102.3 Torr respectively. The inset shows an expanded part around the P(12) transition. The strong rapid passage induced "emission" signal begins to be quenched as the collisional dephasing competes with the rapid passage driving and disappears in trace (d) at *ca*. 25 Torr. Subsequent traces (e) and (f) show a normal mainly Lorentzian pressure broadened lineshape.

22 MHz ns^{-1}. In Fig. 17(a) a broad scan is shown using a path length of 110 m and range of gas pressures of up to 4 mTorr. With a pressure of 4 mTorr in the absorption cell there should be no transmission through the cell, however even under this situation of high absorption there is incomplete attenuation of the laser radiation. There is also a very narrow and strong emission spike corresponding to an effective "transmission" of about 1.8. The observation of the three very weak lines (a)–(c) allows the effects of number density to be checked, since these lines have similar transition dipole moments to the strong lines. (a) and (b) are due to ^{15}N isotopic replacements of one of the two ^{14}N atoms in nitrous oxide and (c) to the second hot band. These lines show similar shapes and intensities to those of the main line at the same number density in the gas cell. In Fig. 17(b) a section of the spectrum around the P(10) line is displayed. In the slowly chirped spectrum the oscillatory structure is almost completely suppressed. The region around the ℓ-doublet of the P(17) line of the first hot band is shown in figure 17(c). The ability of the slow chirp to resolve an ℓ-doublet splitting of 0.005 cm^{-1} shows that the instrumental resolution is close to that set by the calculated transform limited value of 0.0047 cm^{-1}. The calculated resolution of the fast chirp is 0.0125 cm^{-1}, which is insufficient to resolve the doubling. However the recurrence signal seen on the fast chirp is due to the interference between the rapid passage signals generated from the closely spaced doublets, and is similar to an effect seen in NMR spectra.[34]

The oscillatory structure or "wiggles" which accompany the switch from absorption to emission are an indication that rapid passage processes are occurring. These are the infrared

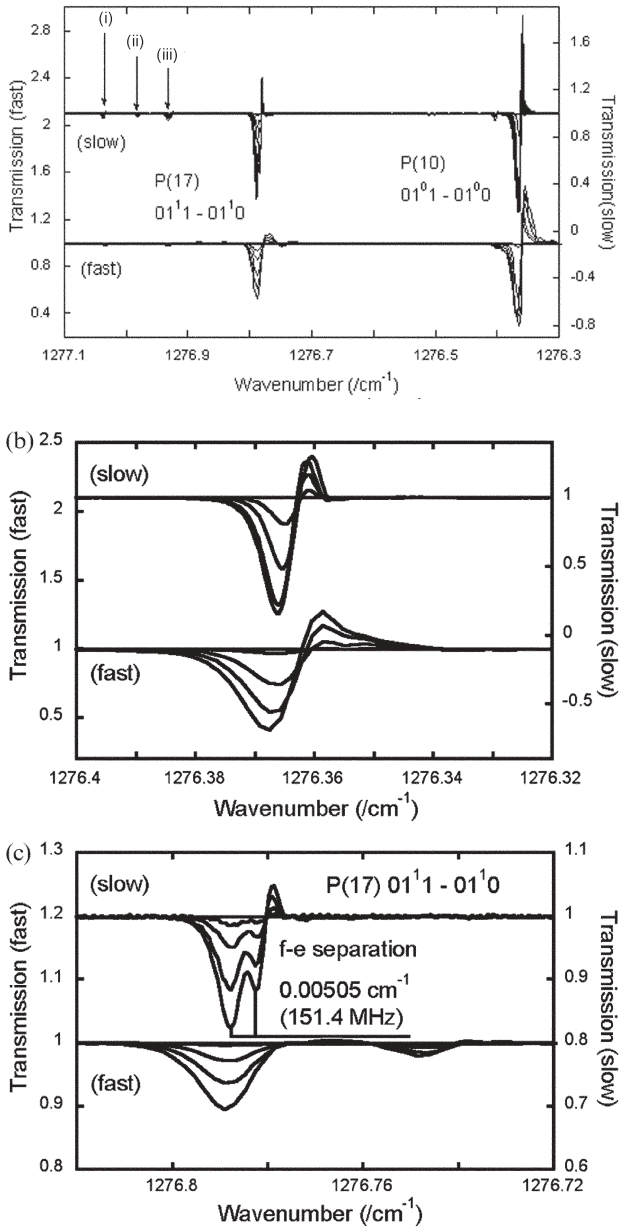

Fig. 17 A comparison of a the rapid passage signals observed from nitrous oxide using a fast chirp (161 MHz ns^{-1}) and a slow chirp (22 MHz ns^{-1}), using a laser pulse duration of 1.5 microseconds and a pulse repetition frequency of 20 kHz averaged for one second. The path length was 110 m. The total range of the comparison is shown in (a). The maximum gas pressure used in (a) is 4 mTorr . Two of the three very weak lines, (i) and (ii) are due to ^{15}N isotopic replacement of one of the two ^{14}N atoms in nitrous oxide, while (iii) arises from the second hot band. (b) a section of the spectrum around the P(10) line to show the partially resolved oscillatory structure of the fast chirp, and the sharp rapid passage signal of the slow chirp, in which there is little evidence for oscillatory structure. The limitation of the resolution of the oscillatory structure of the rapidly chirped laser is set by the transform limit as described earlier. The pressures used are 0.1, 0.25, 0.5 and 0.75 mTorr. (c) The spectrum of the ℓ-doublet of the P(17) line of the first hot band. The ℓ-doubling of 0.005 cm^{-1} is unresolved in the fast chirp (calc. Res. 0.0125 cm^{-1}), but is resolved in the slow chirp (calc. Res. 0.0047 cm^{-1}).

equivalent of wiggles seen after the lines in magnetic field swept NMR spectra. These are due to rapid passage since the rate of frequency sweep is faster than the relaxation times of the system. One of the most complete descriptions of this behaviour in NMR spectra has been given by Ernst.[34] Similar rapid passage signals were observed in gas phase pure rotation microwave spectra by Flygare and his group.[35]

The standard method of treating this type of process is derived from a study of similar effects in frequency swept NMR, the Bloch vector approach.[34] When this is applied to electric dipole transition it is usually called the Optical Bloch, or Maxwell Bloch, approach.[27] The description is based upon the transitions between a lower level, a, and an upper level, b, of a two level system. Assuming that the population of the upper level may decay to the lower level at a rate Γ_{ba}, the lifetime of the upper level, T_1 is then given by $T_1 = 1/\Gamma_{ba}$. If the magnetic or electric dipole moment of the transition from b to a is dephased in a characteristic time T_2, the transition line width in the limit of weak radiation fields is then $\gamma_{ba} = \gamma_2 = 1/T_2$, so that the full width in angular frequency units is $2\gamma_{ba}$. T_1 is known as the transverse relaxation time, and T_2 the longitudinal relaxation time.

In NMR and microwave spectra the transverse (population), T_1 and longitudinal (coherence), T_2, relaxation times are mainly determined by homogeneous processes such a collisions. Since the rapid passage signals observed in the intrapulse QC spectrometer resembled those seen in NMR or microwave spectra, the first attempt at modeling the behaviour of these signals was a development of the models of Ernst[34] and of McGurk *et al.*[35]

When the rapidly swept laser radiation interacts with the molecules the interaction time is determined by the chirp rate of typically *ca.* 20–200 MHz ns^{-1}, and by the homogeneous width of the transition, $\Delta\nu_H$, which for low pressure gases is about 10 MHz. Under these conditions the interaction time is less than 500 ps, and is also less than de-phasing time ($\sim 1/\Delta\nu_H$ $1/\Delta\nu_H > 100$ ns). Under these conditions there is no de-phasing as radiation sweeps through transition and hence there is the potential for rapid passage processes to occur in low pressure gases. This will lead to the coherent transfer of population between levels.

The components of the Bloch vector, u and v are related to the real and imaginary parts of the complex refractive index of the medium respectively, u is the dispersive part and v the absorptive part, and w is related to the population difference between the levels b and a. If one treats one particular vibration–rotation transition as a two level system, the evolution of Bloch vector components u, v, w is then given by

$$\frac{du}{dt} = -\Delta(t)v - \gamma_2 u,\ \frac{dv}{dt} = -\Delta(t)u - \gamma_2 v + \kappa E w$$

$$\frac{dw}{dt} = -\kappa E w - \gamma_1\left(w - w_{eq}\right),\ \Delta(t) = \omega_a - (\omega_i + \alpha t),\ \kappa = \frac{\mu}{\hbar}$$

where $\gamma_1 = 1/T_1$, $\gamma_2 = 1/T_2$, κ is the molecule field coupling constant, and $\Delta(t)$ is the detuning from resonance.

These equations may be integrated numerically in either time or the frequency domain. In order to simplify the problem McCulloch *et al.*[33] made the following assumptions: that there

is a linear chirp across transition, and that there is a constant field across transition of 35 kV m^{-1}. They also assumed a transition dipole moment of 0.175 Debye, and a Rabi frequency of 50 MHz. The assumed de-phasing rate, γ_2, was set at 10 MHz. The initial conditions were taken to be:

$$u(\Delta = -\infty) = 0,\ v(\Delta = -\infty) = 0,\ w(\Delta = -\infty) = -1.$$

When the behaviour of the line is calculated in this way, the simulation, Fig. 18 (a) shows evidence of a large number of rapid oscillations, or wiggles, after the absorptive part, whereas the observed line does not, Fig. 16 and 17.

In order to understand this discrepancy we need to take into account the effects of Doppler broadening. In NMR and microwave spectra the transverse (population), T_1 and longitudinal (coherence), T_2, relaxation times are mainly determined by homogeneous processes. However in the infrared spectra of low pressure gases the Doppler broadening is much larger than the pressure broadening. Hence the signals seen in this region arise from sweeping through an inhomogeneously (Doppler) broadened line.

In an inhomogeneously broadened line the different velocity components will have different resonance frequencies, so that each velocity component will act as an emitter. The total response the sum of all the individual emitters is equivalent to that of a phased array, see Fig. 13(a). When a calculation of this phase delay effect is carried out numerically, the resultant line shape shown below in Fig. 18(b) is very similar to that observed experimentally in Figs. 16 and 17.

The population transfer is also very dependent upon the chirp rate. In Fig. 19. the population transfer is calculated in (a) for a fast chirp rate of 200 MHz ns^{-1}, and in (b) for a much slower chirp rate of 20 MHz ns^{-1}. It can be seen that with a very rapid chirp there is little or no population transfer, but as the rate is slowed, for a fixed value of the driving Rabi frequency, a significant amount of population is transferred. When the chirp is slowed still further eventually a fully inverted population will be produced. This is the limiting case of adiabatic rapid passage. In the absence of collisions the population is transferred completely from the lower state, $w = -1$, to the upper state, $w = 1$.

Although the pulsed lasers have output powers of 5 to 100 mW, these should not be sufficient to cause the large electric fields required for the large Rabi frequencies necessary for the experimental observation of the large rapid passage signals. The increase in the size of the non-linear driving as the gas pressure is increased at constant laser power is similar to that observed when the laser power is increased. At constant laser power the only method of increasing the power density is by reducing the cross sectional area of the beam. In materials with a strong optical nonlinearity this may be caused by self focusing. Since the transition dipole moment and other parameters of nitrous oxide are well determined, as is the laser power, the only free parameter in any numerical simulation of the effects is the degree of self focusing.

Not only can rapid passage effects be observed when using pulsed QC lasers, related signals may be observed when the sweep rate of a CW QC laser is sufficiently rapid, and can be seen in the spectrum of nitrous oxide shown previously in Fig. 3. They may also be observed when a short perturbation current pulse is added at a particular time delay during the scan of a slowly swept CW QC laser through a molecular absorption line. These methods which have been developed by Kelly, and have been applied by Duxbury, Blake and Kelly[36] to study the nonlinear behaviour of absorption lines of NO in

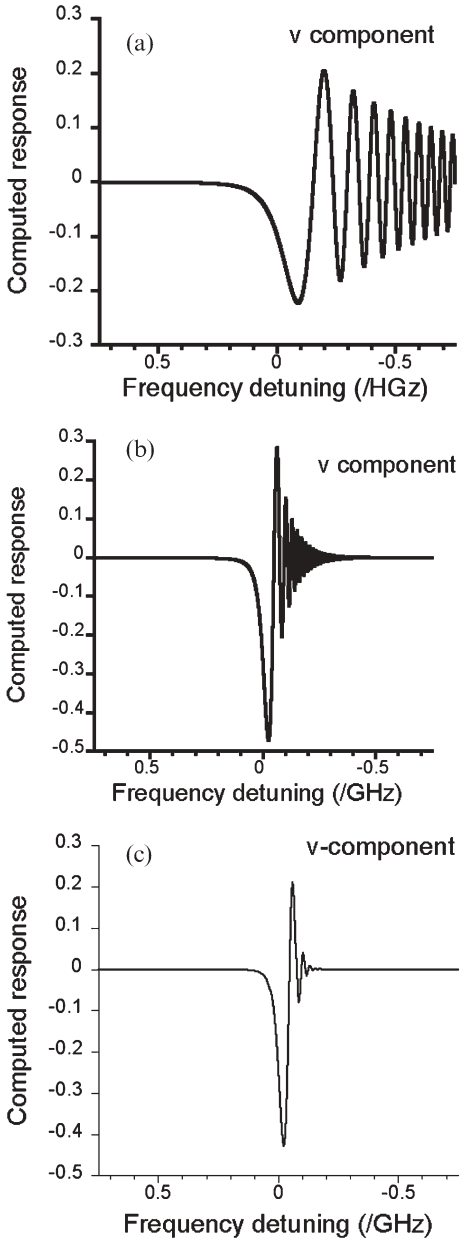

Fig. 18 Calculated rapid passage signals. (a) Using a chirp rate of 200 MHz ns^{-1}, a Rabi frequency of 100 MHz, a T_1 value of 10 MHz and a T_2 value of 100 MHz, but neglecting the inhomogeneous lineshape. (b) Using a chirp rate of 20 MHz ns^{-1}, the other parameters as (a). (c) Allowing for the dephasing arising from the sequential excitation of the successive components of the Doppler broadened line, which were shown schematically in Fig. 13(a). The model calculations used a T_2 value of 10 MHz, a Gaussian half width of 100 MHz, an integration range from −5 to 5 GHz, and a step width of 5 MHz. The oscillatory structure predicted by (b) is now much more strongly damped.

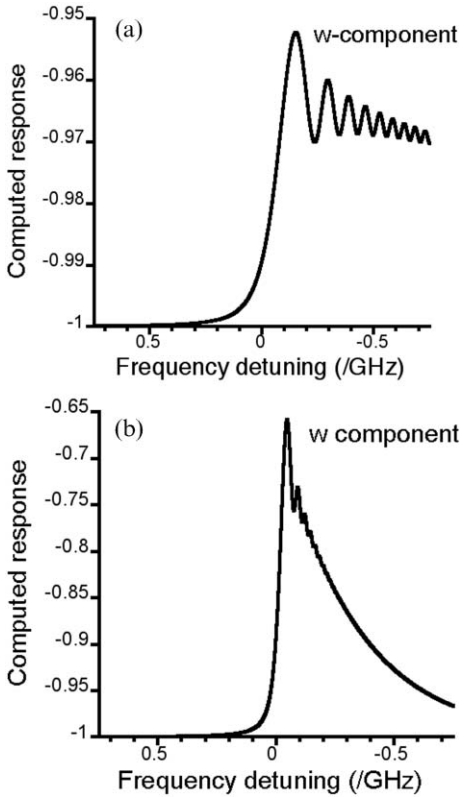

Fig. 19 Population transfer associated with rapid passage. (a) The calculated population difference, the *w*-component of the Bloch vector, as a function of laser detuning using a chirp rate of 200 MHz ns^{-1} and the other parameters as Fig. 18 (a). (b) Calculated *w*-component of the Bloch vector using a chirp rate of 20 MHz ns^{-1} as in Fig. 18(b).

the 5 micron region, and of nitrous oxide in the 8 micron region. These latter experiments have allowed a direct comparison to be made between the behaviour of a strongly absorbing line subject to one strongly saturating rapidly swept field, McCulloch *et al.*[33] and of two fields derived from a modulated CW laser (Duxbury, Blake and Kelly[36]). The fact that large rapid passage effects may be observed using QC laser spectrometers opens up a wide range of possibilities for coherent control experiments using QC lasers.

Future developments

The fabrication of QC lasers is being improved rapidly to allow more efficient lasers to be developed in the mid infrared region. By developing lasers which have much more efficient extraction of heat from the active region, several groups[6,7] have demonstrated recently that continuous operation may be achieved at or slightly above room temperature. When these developments feed into commercially available lasers it will allow continuous operation of QC lasers using electrical cooling, removing their current reliance on cryogenic Dewars.

Other exciting prospect have arisen as a result of the extension of their operating range to the submillimetre (or Terahertz) region near 100 microns, since there are few directly tunable sources which span much of this region. The advent of submillimetre QC laser of steadily increasing wavelength, developed by Köhler *et al.*,[37] and Barbieri *et al*[38] has opened up a variety of possibilities from spectroscopic to imaging. A recent demonstration of the way in which difference between the transmission properties of submillimetre radiation and those of light allows novel images to be obtained may be seen in the recently published submillimetre images of a rats brains by Darmo *et al.*[39] These lasers are also being developed as local oscillators for the next generation of sub-millimetre and far-infrared telescopes. Recent heterodyne beat experiments[40] demonstrate the slow thermal chirp and narrow linewidth of these lasers, which will play an important role in future explorations of astro chemistry and biology.

The final type of recent laser development is that of a broadly tuneable QC laser. The first example of this was demonstrated by Gmachl *et al.*[41] in 2002. More recently a different design, developed by Maulini *et al.*[42] has been shown to have considerable potential to form part of an external cavity tuned QC laser with a tuning range of about a hundred cm^{-1}.

Acknowledgements

The authors are grateful to both the EPSRC and also the NERC for equipment and studentship grants in support of the development of the intra-pulse spectrometer. They are also grateful for the collaboration with J. F. Kelly and T. A. Blake of the Environmental Molecular Science Laboratory (EMSL) of Pacific Northwest National Laboratory (PNNL) and for the use of EMSL by one of us (GD). Finally they would like to thank C. R. Webster, M. S. Taubman and M. S. Zahniser for supplying original versions of some of their spectra.

References

1 E. D. Hinkley, K. W. Knill and F. A. Blum, Infrared spectroscopy with Tunable Lasers, in *Laser Spectroscopy of Atoms and Molecules*, H. Walter ed., Topics in Applied Physics, Springer, Berlin, Heidelberg, New York, 1976, vol. 2, p. 127.
2 Geoffrey Duxbury, *Infrared Vibration-Rotation Spectroscopy; From Free Radicals to the Infrared Sky*, Wiley, Chichester, 2000.
3 F. K. Tittel, D. Richter and A. Freed, Mid-Infrared Laser Applications in Spectroscopy, in *Solid State Infrared Sources*, I. T. Sorokina and K. L. Vodopyanov (Eds.), *Topics Appl. Phys.,* Springer, Berlin, Heidelberg, 2003, vol. 89, pp. 445–516.
4 J. Faist, F. Capasso, D. L. Sivco, C. Sirtori, A. L. Hutchinson and A. Y. Cho, *Science*, 1994, **265**, 553–556.
5 R. F. Kazarinov and R. A. Suris, *Sov. Phys. Semicond.*, 1971, **5**, 707.
6 D. A. Yarekha, M. Beck, S. Blaser, T. Aellen, E. Gini, D. Hofstetter and J. Faist, *Electron Lett.*, 2003, **39**, 1123–1125.
7 J. S. Yu, S. Slivken, L. Doris and M. Razeghi, *Appl. Phys. Lett.*, 2003, **83**, 2503–2505.
8 J. Faist, C. Gmachl, F. Capasso, C. Sirtori, D. L. Sivco, J. N. Baillargeon and A. Y. Cho, *Appl. Phys. Lett.*, 1997, **70**, 2670–2672.
9 J. B. McManus, P. L. Kebabian and M. S. Zahniser, *Appl. Opt.*, 1995, **34**, 3336–3348.
10 S. W. Sharpe, J. F. Kelly, J. M. Hartman, C. Gmachl, F. Capasso, D. L. Sivco, J. N. Baillargeon and A. Y. Cho, *Opt. Lett.*, 1998, **23**, 1396–1398.
11 C. R. Webster, G. J. Flesch, D. C. Scott, J. E. Swanson, R. D. May, W. S. Woodward, C. Gmachl, F. Capasso, D. L. Sivco, J. N. Baillargeon, A. L. Hutchinson and A. Y. Cho, *Appl. Opt.*, 2001, **40**, 321–326.
12 K. Namjou, S. Cai, E. A. Whittaker, J. Faist, C. Gmachl, F. Capasso, D. L. Sivco and A. Y. Cho, *Opt. Lett*, 1998, **23**, 219–221.

13 A. A. Kosterev, R. F. Curl, F. K. Tittel, C. Gmachl, F. Capasso, D. L. Sivco, J. N. Baillargeon, A. L. Hutchinson and A. Y. Cho, *Appl. Opt.*, 2000, **39**, 6866–6872.
14 D. D. Nelson, J. H. Shorter, J. B. McManus and M. S. Zahniser, *Appl. Phys. B*, 2002, **75**, 343–350.
15 M. T. McCulloch, E. L. Normand, N. Langford, G. Duxbury and D. A. Newnham, *J. Opt. Soc. Am. B*, 2003, **20**, 1761–1768.
16 T. Beyer, M. Braun and A. Lambrecht, *J. Appl. Phys.*, 2003, **93**, 3158–3160.
17 R. Bracewell, *The Fourier Transform and Its Applications*, McGraw Hill, New York, 1965.
18 B. M. Gorshunov, A. P. Shotov, I. I. Zasavitsky, V. E. Koloshnikov, Yu. A. Kuritsyn and G. V. Vedeneeva, *Opt. Commun.*, 1979, **28**, 64–68.
19 C. R. Webster and A. J. Heymsfield, *Science*, 2003, **202**, 1742–1745.
20 K. H. Rosenlof, *Science*, 2003, **202**, 1691–1692.
21 R. E. Baren, M. E. Parrish, K. H. Schafer, C. N. Harward, Q. Shi, D. D. Nelson, J. B. McManus and M. S. Zahniser, *Spectrochim. Acta*, 2004, **A60**, 3437–3447.
22 D. D. Nelson, J. B. McManus, S. Urbanski, S. Herndon and M. S. Zahniser, *Spectrochim. Acta*, 2004, **A60**, 3325–3335.
23 M. T. McCulloch, N. Langford and G. Duxbury, *Appl. Opt.*, 2005, **44**, 14.
24 H. Ganser, W. Urban and J. M. Brown, *Mol. Phys.*, 2003, **101**, 545–550.
25 R. G. Brewer, Coherent Optical Spectroscopy, in *Nonlinear Spectroscopy*, Proceedings of the International School for Physics "Enrico Fermi", Course LXIV, Ed. N. Bloembergen, 1977, pp. 87–135.
26 M. M. T. Loy, *Phys. Rev. Lett.*, 1974, **32**, 814–817.
27 R. L. Shoemaker, Coherent Transient Infrared Spectroscopy, in *Laser and Coherence Spectroscopy*, Ed. J. I. Steinfeld, Plenum, New York, 1978, pp. 197–371.
28 M. Mürtz, M. Schaefer, T. George, J. S. Wells and W. Urban, *Appl. Phys. B*, 1995, **60**, 31.
29 J. T. Remillard, D. Uy, W. H. Weber, F. Capasso, C. Gmachl, A. L. Hutchinson, D. L. Sivco, J. N. Baillargeon and A. Y. Cho, *Opt. Express*, 2000, **7**, 243–248.
30 J. F. Kelly, R. S. Disselkamp, R. L. Sams, T. A. Blake, S. W. Sharpe, D. A. Richter and A. Fried, *Proc. SPIE*, 2002, **4817**, 43–72.
31 M. S. Taubman, T. L. Myers, B. D. Cannon and R. M. Williams, *Spectrochim. Acta*, 2004, **A60**, 3457–3468.
32 J. Ye, L. S. Ma and J. L. Hall, *J. Opt. Soc. Am. B*, 1998, **15**, 6.
33 M. T. McCulloch, S. Wright, N. Langford and G. Duxbury, (in preparation 2005).
34 R. R. Ernst, Sensitivity Enhancement in Magnetic Resonance, *Advances in Magnetic Resonance*, Academic Press, 1966, vol. 2, pp. 1–135.
35 J. C. McGurk, T. G. Schmalz and W. H. Flygare, *J. Chem. Phys.*, 1974, **60**, 4181.
36 G. Duxbury, J. F. Kelly and T. A. Blake, (in preparation, 2005).
37 R. Köhler, A. Tredicucci, F. Beltram, H. E. Beere, E. C. Linfield, A. G. Davies, D. A. Ritchie, R. C. Lotti and F. Rossi, *Nature*, 2002, **417**, 156–159.
38 S. Barbieri, J. Alton, H. E. Beere, J. Fowler, E. C. Linfield and D. A. Ritchie, *App. Phys. Lett.*, 2004, **85**, 1674–1676.
39 J. Darmo, V. Tamosiunas, G. Fasching, J. Kröll, K. Unterrrainer, M. Beck, M. Giovannini, J. Faist, C. Kremser and P. Debbage, *Opt. Express*, 2004, **9**, 1879–1884.
40 A. Barkan, F. K. Tittel, D. M. Mittelman, R. Dengler, P. H. Siegel, G. Scalari, L. Ajili, J. Faist, H. E. Beere, J. Fowler, E. C. Linfield and D. A. Ritchie, *Optics Lett.*, 2004, **29**, 575–577.
41 C. Gmachl, D. L. Sivco, R. Colombelli, F. Capasso and A. Y. Cho, *Nature*, 2002, **415**, 883.
42 R. Maulini, M. Beck, J. Faist and E. Gini, *Appl. Phys. Lett.*, 2004, **84**, 1659–1661.

